British Journal of Pharmacology

DOI:10.1111/bph.12611
www.brjpharmacol.org

RESEARCH PAPER

Salidroside exerts angiogenic and cytoprotective effects on human bone marrow-derived endothelial progenitor cells via Akt/mTOR/p70S6K and MAPK signalling pathways

Yubo Tang[1,2]*, Corina Vater[1]*, Angela Jacobi[1], Cornelia Liebers[1], Xuenong Zou[3] and Maik Stiehler[1]

[1]*Centre for Translational Bone, Joint and Soft Tissue Research, Medical Faculty and University Centre for Orthopaedics and Trauma Surgery, University Hospital Carl Gustav Carus at Technische Universität Dresden, Dresden, Germany,* [2]*Department of Pharmacy, the First Affiliated Hospital of Sun Yat-sen University, Guangzhou, China, and* [3]*Department of Spinal Surgery, the First Affiliated Hospital of Sun Yat-sen University, Guangzhou, China*

Correspondence
Maik Stiehler, Centre for Translational Bone, Joint and Soft Tissue Research, Medical Faculty and University Centre for Orthopaedics and Trauma Surgery, University Hospital Carl Gustav Carus at Technische Universität Dresden, Fetscherstrasse 74, D-01307 Dresden, Germany. E-mail: Maik.stiehler@uniklinikum-dresden.de; Xuenong Zou, Department of Spinal Surgery, the First Affiliated Hospital of Sun Yat-sen University, 510080 Guangzhou, China. E-mail: zxnong@hotmail.com

*These authors contributed equally to the work.

Keywords
endothelial progenitor cell; salidroside; angiogenesis; reactive oxygen species; apoptosis; Akt/mTOR/p70S6K; MAPK

Received
24 July 2013
Revised
12 January 2014
Accepted
23 January 2014

BACKGROUND AND PURPOSE

With the increase of age, increased susceptibility to apoptosis and senescence may contribute to proliferative and functional impairment of endothelial progenitor cells (EPCs). The aim of this study was to investigate whether salidroside (SAL) can induce angiogenic differentiation and inhibit oxidative stress-induced apoptosis in bone marrow-derived EPCs (BM-EPCs), and if so, through what mechanism.

EXPERIMENTAL APPROACH

BM-EPCs were isolated and treated with different concentrations of SAL for up to 4 days. Cell proliferation, migration and tube formation ability were detected by DNA content quantification, transwell assay and Matrigel-based angiogenesis assay. Gene and protein expression were assessed by qRT-PCR and Western blot respectively.

KEY RESULTS

Treatment with SAL promoted cellular proliferation and angiogenic differentiation of BM-EPCs, and increased VEGF and NO secretion, which in turn mediated the enhanced angiogenic differentiation of BM-EPCs. Furthermore, SAL significantly attenuated hydrogen peroxide (H_2O_2)-induced cell apoptosis, reduced the intracellular level of reactive oxygen species and restored the mitochondrial membrane potential of BM-EPCs. Moreover, SAL stimulated the phosphorylation of Akt, mammalian target of rapamycin and p70 S6 kinase, as well as ERK1/2, which is associated with cell migration and capillary tube formation. Additionally, SAL reversed the phosphorylation of JNK and p38 MAPK induced by H_2O_2 and suppressed the changes in the Bax/Bcl-xL ratio observed after stimulation with H_2O_2.

CONCLUSIONS AND IMPLICATIONS

These findings identify novel mechanisms that regulate EPC function and suggest that SAL has therapeutic potential as a new agent to enhance vasculogenesis as well as protect against oxidative endothelial injury.

Abbreviations

BM-EPCs, bone marrow-derived endothelial progenitor cells; DPI, diphenyliodonium; eNOS, endothelial NOS; VEGFR2 (KDR), kinase insert domain receptor; L-NAME, N^G-nitro-L-arginine methyl ester; MMP, mitochondrial membrane potential; mTOR, mammalian target of rapamycin; Nox4, NADPH oxidase 4; p70S6K, ribosomal protein S6 kinase; PECAM-1, platelet endothelial cell adhesion molecule; SAL, salidroside; VE-cadherin, vascular endothelial cadherin; vWF, von Willebrand factor

Introduction

Endothelial progenitor cells (EPCs) are a heterogeneous subpopulation of bone marrow mononuclear progenitor cells with the potential to differentiate into the endothelial lineage. EPCs can form endothelial colonies *in vitro* and contribute to revascularization *in vivo* (Asahara *et al.*, 1997; Shi *et al.*, 1998; Iwakura *et al.*, 2003; Asahara and Kawamoto, 2004; Tepper *et al.*, 2005). Transplantation of EPCs into severely ischaemic tissues has been shown to induce angiogenesis and to increase functional blood supply (Gunsilius *et al.*, 2000; Kalka *et al.*, 2000; Kawamoto *et al.*, 2002). Bone marrow-derived EPCs (BM-EPCs) represent a promising alternative cell source to enhance vasculogenesis in the field of regenerative medicine and have already been successfully used to support neovascularization after myocardial infarction and limb ischaemia (Iwakura *et al.*, 2006; Palladino *et al.*, 2012). Moreover, EPCs can enhance site-specific bone repair (Rozen *et al.*, 2009; Atesok *et al.*, 2010). However, clinical studies have reported that with an increase in age, a higher risk of apoptosis and accelerated senescence may contribute to the observed numerical proliferative and functional impairment of EPCs (Scheubel *et al.*, 2003; Hoetzer *et al.*, 2007; Kushner *et al.*, 2009). This in turn is associated with an increased risk of vascular disease and prolonged and often complicated recovery from acute vascular events (Vasa *et al.*, 2001; Scheubel *et al.*, 2003; Dimmeler and Zeiher, 2004). Furthermore, reduced tissue levels of EPCs and functional impairment of endothelium are often observed in patients with diabetes and cardiovascular disease (De Vriese *et al.*, 2000; Vasa *et al.*, 2001). Hence, attention has increasingly been paid to enhance mobilization and differentiation of EPCs for therapeutic purposes.

A large body of evidence indicates that in traditional Chinese medicine (TCM) a plethora of herbs and herbal extracts are effective in the treatment of vascular diseases such as chronic wounds, diabetic retinopathy and rheumatoid arthritis (Shu *et al.*, 2010; Zhai *et al.*, 2013). Thus, it seems rational to explore these medicinal plants as potential sources of novel angiomodulatory factors. Rhodiola is a widely used TCM herb that has been shown to improve cognitive function, reduce mental fatigue, promote free radical mitigation, and enhance learning and memory (Darbinyan *et al.*, 2000; Spasov *et al.*, 2000; Shevtsov *et al.*, 2003; De Bock *et al.*, 2004). Rhodiola extracts exert antiarrhythmic activity, show anti-inflammatory and neuroprotective effects, and prevent ischaemia–reperfusion-induced ventricular tachycardia (Maslov *et al.*, 2009; Qu *et al.*, 2012; Sun *et al.*, 2012). Salidroside (SAL), the major phenylpropanoid glycoside and pharmacological active constituent derived from Rhodiola, possesses potent anti-apoptotic effects in various cell types, for example neurons and cardiomyocytes as well as in preclinical disease models, such as acute myocardial infarction in rats (Zhong *et al.*, 2010; Qu *et al.*, 2012). Furthermore, SAL attenuated early ischaemic brain injury, improved acute behavioural dysfunctions caused by focal cerebral ischaemia, and protected against cerebrovascular injuries (Shi *et al.*, 2012). The potential efficacy of SAL on BM-EPCs may be additionally used for the treatment of ischaemic diseases and bone defects. However, as this strategy has not been evaluated so far, the present study was designed to (i) evaluate the potential angiomodulatory and anti-oxidant effects of SAL on BM-EPCs and to (ii) investigate the molecular mechanisms involved.

Here we demonstrated that SAL strongly enhances both cellular proliferation and angiogenic differentiation of BM-EPCs, as well as preventing hydrogen peroxide (H_2O_2)-induced cell death. Furthermore, we provide evidence that these effects involve the Akt/mammalian target of rapamycin (mTOR)/ribosomal protein S6 kinase (p70S6K) and MAPK signalling pathways.

Methods

Reagents

The purity of SAL (Tauto Biotec, Shanghai, China) used for *in vitro* experiments was ≥99%. SAL was dissolved in DMSO (Sigma-Aldrich, St. Louis, MO, USA) to a stock concentration of 100 mM and then aliquoted and stored at –20°C. The amount of DMSO added to the cell culture was less than 0.8% in all cases. Human basic fibroblast growth factor (bFGF) was purchased from Peprotech (London, UK) and used as a positive control.

Isolation and cultivation of BM-EPCs

Informed consent for bone marrow collection was obtained from healthy volunteers (eight donors, age range 20–51 years, mean age 28.6 years) and all procedures were performed in accordance with the guidance and approval of the local institutional review board (approval no. EK263122004). The procedures for isolation, cultivation and identification of human BM-EPC cultures followed previously published methods (Tang *et al.*, 2011). Briefly, mononuclear cells were collected by density gradient centrifugation using Ficoll-Paque™ Premium (1.077; GE Healthcare, San Francisco, CA, USA). The isolated cells were cultivated in flasks coated with 25 $\mu g \cdot mL^{-1}$ human fibronectin (BD Biosciences, San Jose, CA, USA) and

induced by endothelial cell growth medium 2 (EGM-2, PromoCell, Heidelberg, Germany) at 37°C with 5% CO_2 in a humidified incubator at a density of 5×10^6 cm^{-2}. After 72 h in culture, non-adherent cells were removed by washing with new medium. Thereafter, medium was changed every third day of cultivation. After 1 week of cultivation BM-EPCs were characterized by immunofluorescence staining and flow cytometry. All cells used in our study were cultivated with EGM-2 at passages 3–5.

Analysis of cellular proliferation

BM-EPCs were seeded at a density of 6×10^3 cells per well in 96-well plates, cultured with EGM-2 for 24 h followed by a starvation period of 24 h in EGM-2 without FBS. Then medium was replaced by fresh non-FBS EGM-2 containing different concentrations of SAL and cells were incubated for an additional period of 1, 2 and 4 days. After samples were washed once with PBS and lysed in PBS containing 0.1% Triton X-100 (Sigma-Aldrich) for 50 min, DNA content was determined using the Quant-iT PicoGreen dsDNA Assay Kit (Life Technologies GmbH, Darmstadt, Germany) according to the manufacturer's instructions. Fluorescence was measured using a fluorescent microplate reader (SpectraFluorPlus, Tecan, Männedorf, Switzerland) at 480/520 nm wavelength. Triplicates were used for each experimental unit.

Cell migration (chemotaxis) assay

Here we have adopted two methods to investigate the SAL-induced migratory activity of human EPCs in a transwell assay (Millipore, Zug, Switzerland; 6.5 mm diameter, 8 μm pore size filters). Firstly, cells were cultivated for 7 days with EGM-2, trypsinized and counted. A fraction of 8×10^4 cells in 200 μL non-FBS EBM-2 were seeded into the upper chamber while 700 μL of culture medium containing 1% FBS and different concentrations of SAL were placed in the lower chamber. The EPCs were allowed to migrate for 4 h at 37°C in the tissue culture incubator. Secondly, EPCs that were treated with SAL for 48 h were trypsinized, washed and resuspended in EBM-2 without FBS. A fraction of 1×10^5 cells in 200 μL EBM-2 was added to the top chamber of a transwell and 700 μL EBM-2 with 5% FBS were added to the bottom chamber. Cells were allowed to migrate for 2 h. To quantify the number of migrated EPCs on the membrane, the upper side of the membrane was washed carefully with cold PBS and the remaining cells on this side were removed with a cotton swab. Transwell membranes were stained with Alexa Fluor 488® phalloidin in PBS (Life Technologies GmbH) and the migrated cells were examined using an inverted fluorescence microscope (Apotome, Carl Zeiss, Oberkochen, Germany). All experiments were performed at least in triplicate with cells counted in 10 random fields of view.

Cell adhesion assay

Cell–matrix adhesion assay. Cell–matrix adhesion assay using human BM-EPCs was performed as described previously (Tang *et al.*, 2011). Briefly, 96-well plates were coated with 25 $\mu g \cdot mL^{-1}$ human fibronectin (BD Biosciences, Heidelberg, Germany) for 1 h. Human BM-EPCs at 1×10^4 cells per well in EGM-2 were plated onto fibronectin-coated 96-well culture plates and incubated for 30 min at 37°C. After washing twice with PBS, adherent cells were fixed with 4% paraformaldehyde, stained with Hoechst 33258 (Invitrogen, Darmstadt, Germany), and visualized under a fluorescence microscope (ApoTome). Additionally, adherent cells were lysed with Triton X-100 and the DNA content was determined using the Quant-iT PicoGreen dsDNA Assay Kit. Representative results of five independent experiments are shown.

Cell–cell adhesion assay. To characterize the possible effect of SAL on cell–cell adhesion, EPCs were grown overnight to a confluent monolayer in EGM-2 and labelled with Hoechst 33258. In addition, EPCs from the same donor were treated with SAL for 48 h and fluorescence-labelled with calcein acetoxymethyl (AM; Molecular Probes, Invitrogen, CA, USA) for 1 h at 37°C followed by washing with PBS. These cells were then plated onto the established cell monolayer (acceptor cells). Attachment and spreading of the plated cells were monitored and recorded after 20 min by fluorescence microscopy. Quantification of intercellular adhesion was performed by counting the number of cells per microscopic field of view that remained attached after three gentle washing steps with PBS.

Matrigel-based capillary-like tube formation assay

The effect of SAL on morphogenesis and tube formation capacity of EPCs was investigated using the capillary tube formation assay on Matrigel basement membrane matrix (ECMatrix™, BD Biosciences, Heidelberg, Germany). Briefly, ECMatrix™ solution was thawed on ice overnight, mixed with 10× ECMatrix™ diluents and placed in a 96-well tissue culture plate (50 μL per well) at 37°C for 1 h to allow the matrix solution to solidify. A fraction of 1.2×10^4 cells per well were seeded on a Matrigel-precoated 96-well plate. Tube formation was observed under an inverted light microscope (Carl Zeiss). Five independent fields were assessed for each well and the average numbers of tubes per 40× magnified field were determined.

ELISA

The levels of VEGF secreted by BM-EPCs into the medium were measured using a commercially avaliable ELISA kit (Peprotech, Rocky Hill, NJ, USA) according to the manufacturer's instructions. Cell culture supernatants were harvested 24 h and 48 h after stimulation with SAL and frozen for later analysis. The absorbance at 405 nm was measured with a microplate reader and all samples were tested in triplicate.

Measurement of NO production of bone marrow derived EPCs (BM-EPCs)

Accumulated nitrite (NO_2^-) generated from cell-released NO in culture supernatants was determined using a spectrophotometric assay based on the Griess reaction. In brief, adherent cells were stimulated with SAL for 2, 5, 8 and 10 days, and cell culture supernatants were collected to demonstrate any time-dependent effect. Supernatants were converted to nitrite by nitrate reductase followed by the Griess reagent (1% sulfanilamide – 0.1 % N-1-naphthyl-ethylenediamine dihydrochloride in 2.5% phosphoric acid) to convert nitrite to a deep purple azo compound. For determination of this compound

the absorbance at 540 nm was measured with a microplate reader and all samples were tested in triplicate.

Cellular viability and lactate dehydrogenase (LDH) release assay

BM-EPCs were treated with SAL or basal medium for 48 h followed by incubation with 1 mM H_2O_2 for 6 h to induce oxidative stress. Cell numbers were determined by DNA quantification as described earlier. Cells incubated without SAL (in EBM-2 only) served as the control group.

LDH is a stable cytosolic enzyme present in all cell types. The cellular viability can be measured in terms of LDH released from dead cells into the supernatant upon rupture of cell membrane. For this purpose, CytoTox 96® Non-Radioactive cytotoxicity assay kit (Promega, Madison, WI, USA) was employed according to the manufacturer's instructions. Briefly, 100 µL of lysis solution were added to the wells containing the untreated control cells before the assay to induce maximum LDH release. To define the LDH content 50 µL supernatant with 50 µL of substrate solution were mixed in 96-well plates. After 30 min incubation at room temperature (RT) in the dark, the enzymatic reaction was stopped with 50 µL stop solution. The absorbance was measured spectrophotometrically at 490 nm using a microplate reader. The percentage of cytotoxicity was calculated according to the following equation:

$$\text{Percentage of cytotoxicity} = \frac{\text{Absorbance of experimental samples}}{\text{Absorbance of maximum LDH release}} \times 100\%$$

Assessment of intracellular reactive oxygen species (ROS) and superoxide production

Intracellular ROS measurement by dichlorofluorescein (DCF). The assessment of ROS involves the use of 2′,7′-DCF diacetate (DCFH-DA; Sigma-Aldrich), which is a stable non-fluorescent molecule that readily crosses cell membranes and is hydrolysed by intracellular esterases to form non-fluorescent DCFH. DCFH is then rapidly oxidized in the presence of ROS into highly fluorescent DCF. Cells were incubated in fresh EBM-2 containing 20 µM DCFH-DA for 30 min at 37°C. After removal of the DCFH–DA-containing medium, ROS formation was stimulated by H_2O_2 (final concentration: 1 mM) for 6 h at 37°C. Before and 6 h after H_2O_2 addition, the fluorescence levels of the samples were measured using a fluorescence microplate reader with the excitation and emission wavelengths set at 488 and 525 nm respectively.

Superoxide measurement by dihydroethidium (DHE). Superoxide generation causes oxidation of DHE into ethidium bromide, which binds to DNA in the nucleus and fluoresces reddish. EPCs were treated with H_2O_2 in the presence or absence of SAL as described earlier. The medium was then replaced by PBS containing DHE (10 µM) followed by an incubation for 30 min at 37°C. The intensity of DHE fluorescence was determined by fluorescence microplate readings and images were collected using a fluorescence microscope and analysed by Zeiss Imaging System.

Determination of NADPH oxidase activity

NADP and NADPH were measured using an Amplite Fluorimetric NADP/NADPH Assay kit (AAT Bioquest, Inc., Sunnyvale, CA, USA). Cells treated with SAL as well as untreated cells were lysed with 0.5% Triton-X100 for 10 min at RT and then mixed with 50 µL NADPH reaction mixture to a total volume of 100 µL per well. After incubation for 90 min at RT, absorbance was monitored at 575 nm.

Measurement of mitochondrial membrane potential (MMP)

Measurement of the MMP ($\Delta\Psi m$) was performed by loading cells with 5 µM Rhodamine123 (Sigma-Aldrich, Steinheim, Germany), a cationic lipophilic fluorochrome that can be taken up by mitochondria in proportion to the $\Delta\Psi m$. After 20 min incubation in the dark, the cells were washed twice with PBS immediately followed by fluorescence reading at 507/529 nm (ex/em).

Calcein AM/propidium iodide (PI) cellular viability assay

Cellular viability was determined using a calcein AM/PI (Sigma-Aldrich, St. Louis, MO, USA) dual-staining assay. The cell-permeant nonfluorescent calcein AM is converted by intracellular esterases into intensely fluorescent calcein producing a uniform green fluorescence in living cells. PI enters cells with damaged membranes and binds to nucleic acids producing a bright red fluorescence in non-viable cells. After SAL stimulation for 48 h, the cell cultures were treated with or without 1 mM H_2O_2 for 6 h. Subsequently, culture medium was removed and cells were rinsed gently twice with warm PBS, while avoiding agitating the cells. Then 2 µM calcein AM and 15 $\mu g \cdot mL^{-1}$ PI in 100 µL PBS were added to each culture well followed by incubation for 30 min at 37°C. Fluorescence was assessed using a fluorescence microscope.

Apoptosis assay by flow cytometry analysis

BM-EPCs were seeded in six-well plates and allowed to attach for 24 h. After 48 h of treatment with SAL (40 and 80 µM) and 6 h of induction by H_2O_2 as detailed earlier, cell apoptosis was assessed by Annexin A5- fluorescein isothiocyanate (annexin V-FITC) apoptosis detection kit following the manufacturer's instructions (Miltenyi, Bergisch Gladbach, Germany). Briefly, the cells were gently trypsinized, washed with PBS, re-suspended in binding buffer and incubated with annexin V-FITC and PI at RT in the dark for 10 min. Flow cytometric analysis was performed using a LSRII system (BD Biosciences™) and FlowJo software (Tree Star, Inc., Ashland, OR, USA).

RNA isolation, cDNA synthesis and qRT-PCR procedure

Total RNA was isolated by using RNeasy Mini Kit (QIAGEN, Hilden, Germany). Total RNA (300 ng) from each sample was subjected to reverse transcription using a cDNA reverse transcription kit (Applied Biosystems, Foster City, CA, USA) according to the manufacturer's protocol. The ABI Prism 7500 fast Sequence Detection System (Applied Biosystems) with Two Step TaqMan® Fast Universal PCR Master Mix

(Applied Biosystems) was used for all PCR experiments. The reactions were performed according to the manufacturer's instructions with minor modifications. Specific primer-probe sets for VEGF, its receptor VEGFR2 (also known as kinase insert domain receptor, KDR; see Alexander *et al.*, 2013), vascular endothelial cadherin (VE-cadherin), von Willebrand factor (vWF), platelet endothelial cell adhesion molecule (PECAM-1), NADPH oxidase 4 (Nox4), STAT-3 and endothelial NOS 3 (eNOS) were purchased from Applied Biosystems. Each PCR run was performed in triplicate including negative control samples containing master mix, primers and probes as described earlier, but no cDNA template. Thermal cycling conditions of the ABI 7500 fast were: 95°C for 20 s for predenaturation, then 40 cycles of 95°C for 3 s, and finally 60°C for 30 s each. Data were normalized to GAPDH expression and fold change was calculated by the $2^{-\Delta\Delta CT}$ method.

Western blotting

Briefly, cells were washed twice with PBS, sonicated in RIPA buffer (Santa Cruz Biotech, Santa Cruz, CA, USA) and homogenized. Debris was removed by centrifugation at 12 000× *g* at 4°C for 10 min and protein concentration was determined using the BCA Protein assay kit according to the manufacturer's instructions (Thermo Fisher Scientific, Rockford, IL, USA). Samples containing 30 μg of protein were separated by electrophoresis on SDS-PAGEs and transferred to PVDF membranes by electroblotting. The membranes were then blocked by incubating with 5% BSA in 20 mM Tris-HCl, 150 mM NaCl, pH 7.5 (TBS) buffer for 1 h followed by incubation with primary antibodies against PCNA, p-Akt, Akt, p-mTOR, m-TOR, p-p70S6K, p70S6K, p-ERK1/2, ERK1/2, p-JNK, JNK, p-p38 MAPK, p38 MAPK, Bcl-xL (Cell Signaling Technology, Danvers, MA, USA) and GAPDH under gentle agitation overnight at 4°C. Proteins were detected using enhanced chemiluminescence with HRP conjugated appropriate secondary antibodies (Cell Signaling Technology). The values of band intensities were quantified by Quantity One 4.6.2 software (Bio-Rad Laboratories, Hercules, CA, USA) to the respective protein loading controls. All immunoblots are representative of at least three independent experiments.

Statistical analysis

Numerical data are presented as the means ± SD from at least three individual experiments with cells from different donors, unless otherwise indicated. Statistical comparisons between groups were performed by one-way ANOVA followed by Student's *t*-test using the Statistical Package for the Social Sciences (SPSS) 16.0 software package (SPSS Inc., Chicago, IL, USA). Statistical significance was established at $*P < 0.05$, $**P < 0.01$ versus the indicated group.

Results

SAL promotes the proliferation of BM-EPCs

To assess the pro-angiogenic property of SAL *in vitro*, we first examined the effect of SAL on cellular proliferation. Human BM-EPCs were treated with varying concentrations of SAL for 24, 48 and 96 h, and cell numbers were assessed by DNA quantification with bFGF serving as positive control. As shown in Figure 1A, cell numbers were increased after incubation with SAL for 48 h at the concentration of 20, 40 and 80 μM. The protein expression of PCNA was also enhanced by 48 h incubation with SAL by 20, 40 and 80 μM (Figure 1B and C). However, no significant effect on cellular proliferation was found at 24 h and 96 h treatment with SAL.

SAL increases cell recruitment ability

EPCs lining the lumina of blood vessels are important elements in blood vessel formation, and directed migration of EPCs is a key angiogenic process. To investigate the effects of SAL-driven motility of BM-EPCs, transwell experiments were performed. When SAL was added to the lower chamber compartment, cells showed a remarkably increased ability to migrate in response to SAL (Figure 2A and B) in a dose-dependent manner, with promotion first occurring at 40 μM (2.59 ± 0.07-fold) and more pronounced at 80 μM (3.05 ± 0.10-fold). The experiments involving pretreatment of EPCs with SAL that were used to measure the ability of SAL to trigger innate cell recruitment ability showed that cell migration increased significantly at 80 μM SAL compared with non-treated cells (Figure 2C and D, $P < 0.01$).

SAL enhances cell adhesion to extracellular matrix (ECM) and decreases cell–cell adhesion

To evaluate whether SAL affects cell–matrix adhesion human fibronectin was used as ECM model. SAL-treated cells attached more readily to the ECM (1.95 ± 0.14-fold and 1.98 ± 0.10-fold increase at 40 and 80 μM SAL, respectively) compared with the control ($P < 0.01$, Figure 3A and B). However, we did not observe significant intergroup differences concerning the numbers of attached cells after 90 min adherence. To investigate whether SAL affects cell–cell adhesion of BM-EPCs, we examined the adherence of SAL-stimulated cells to untreated EPCs. SAL treatment resulted in significantly less adherent EPCs. This effect became apparent at 20 μM and peaked at 80 μM SAL (Figure 3C and D). In summary, SAL provoked the cell adhesive ability to ECM, while it diminished the capacity of cell–cell adhesion.

SAL augments capillary tube formation of BM-EPCs in vitro

An *in vitro* angiogenesis assay was used to investigate the capillary tube formation being a key function of EPCs. To determine whether SAL affects the ability of EPCs to form capillary-like tubes, EPCs were seeded on Matrigel™ and examined for tube formation microscopically. After an 18 h incubation on the gel, the presence of both 20, 40 and 80 μM SAL (Figure 4B) significantly increased the number of sprouting tubules by 250 ± 17.5%, 350 ± 18.8% and 525 ± 10.4% as compared with untreated EPCs. Thus SAL strongly enhanced the ability of EPCs to form tube-like structures.

SAL increases VEGF secretion and NO production in BM-EPCs

In the light of the important role of VEGF and NO in the regulation of angiogenesis and cell function, we evaluated VEGF secretion and NO production in supernatants of

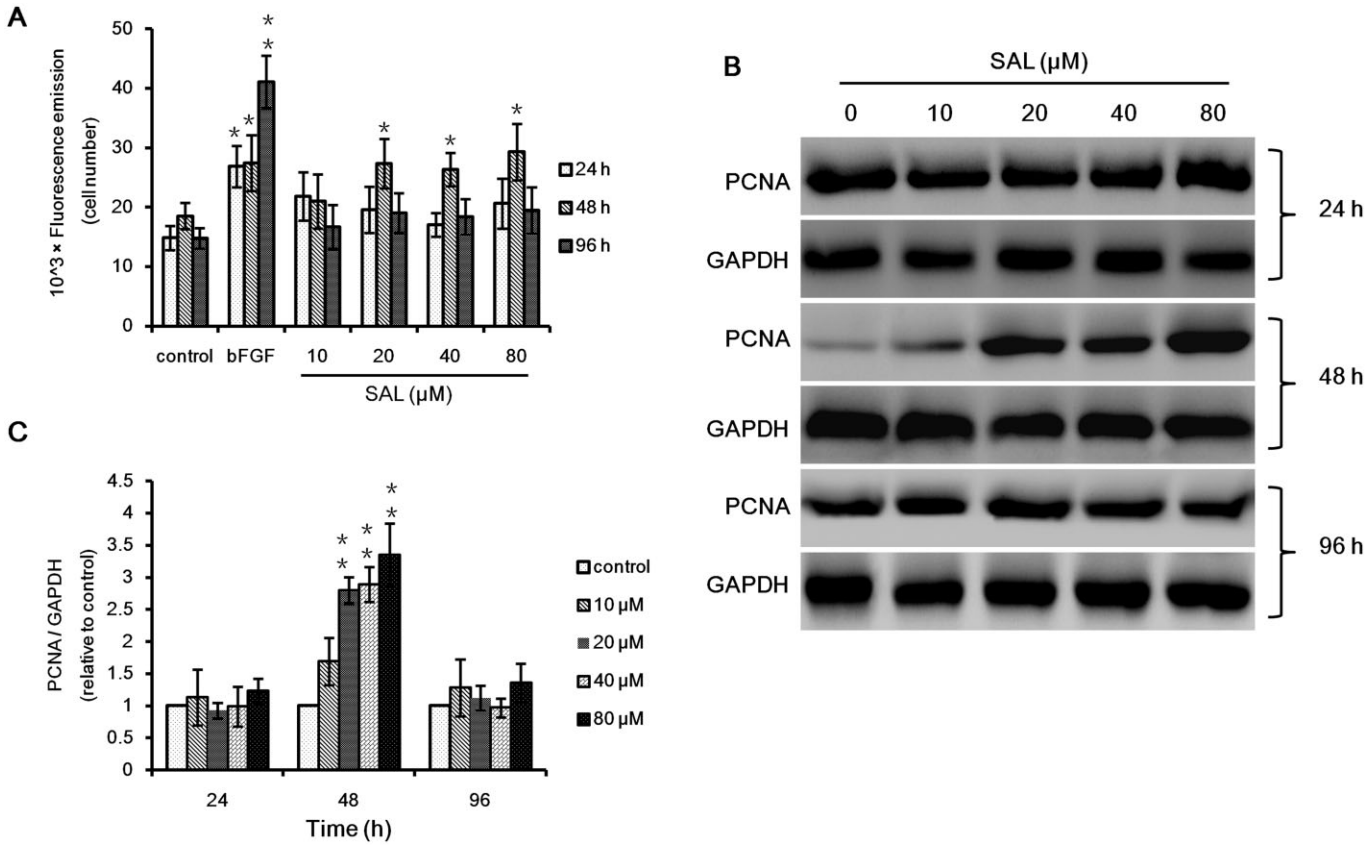

Figure 1

Effect of SAL on cellular proliferation of BM-EPCs. (A) Cells were treated with 0 (control), 10, 20, 40 and 80 μM SAL for 24, 48 and 96 h followed by DNA quantification to determine cellular proliferation, $n = 5$. (B) PCNA expression was measured by Western blot. The immunoblots shown are representative of at least three independent experiments with comparable results. (C) Densitometric analysis of band intensities of PCNA normalized to GAPDH is shown. Data are shown as mean ± SD, $^*P < 0.05$, $^{**}P < 0.01$ versus control group.

BM-EPCs treated with or without SAL. Over periods of 24 h and 48 h incubation, SAL at both 40 and 80 μM enhanced VEGF secretion by 11.3% (24 h, 40 μM), 17.5% (24 h, 80 μM), 18.9% (48 h, 40 μM) and 21.0% (48 h, 80 μM) (Figure 5A). Furthermore, NO production of EPCs increased significantly when cells were stimulated by SAL for 2, 5, 8 and 10 days (Figure 5B). These findings suggest that the enhanced tube-formation ability of EPCs induced by SAL is mediated by increased VEGF and NO production. Moreover, we used N^G-nitro-L-arginine methyl ester (L-NAME), a selective inhibitor of NOS, to examine the role of NO underlying the angiogenic effect of SAL. As shown in Figure 5C, 10 μM L-NAME significantly inhibited SAL-induced NO production after 2 days incubation. Furthermore, the promotion effect of SAL on migration and capillary tube formation ability on EPCs was suppressed by L-NAME (Figure 5D and E). These results imply that endothelium-derived NO plays a key role in the process of blood vessel formation.

SAL inhibits H_2O_2-induced cell death

To assess the influence of SAL on H_2O_2-induced cell death, BM-EPCs were pretreated by 40 and 80 μM SAL followed by stimulation with 1 mM H_2O_2 for 6 h. Then cells were double-stained with calcein-AM/PI and evaluated by observation using fluorescence microscopy. While in the absence of H_2O_2, nearly all cells were alive, the addition of 1 mM H_2O_2 significantly increased the rate of cell death, as was shown by contraction and nuclear membrane creasing. In contrast, an increase in cell viability was observed as evidenced by a reduced fraction of dead cells visualized by Live/Dead assay. Furthermore, the cells retained good morphology without cytoplasm injury (Figure 6A), indicating a protective effect of SAL from H_2O_2-induced cell death.

As shown in Figure 6B, 48 h preincubation with 40 μM and 80 μM SAL dose-dependently attenuated the H_2O_2-induced cell death by 33.6 and 47.0% respectively. Furthermore, the rate of cytotoxicity significantly increased to 42.1% after exposure to H_2O_2 that evidenced by elevated level of LDH (Figure 6C). The cytotoxic effects of H_2O_2 were significantly attenuated by the pretreatment of 80 μM SAL with the cytotoxic rate of 29.9%, but not in the control group. These results demonstrated that SAL can protect BM-EPCs against H_2O_2-induced cell damage.

SAL suppresses H_2O_2-induced production of ROS and NADPH expression

As shown in Figure 6D and E, when compared with BM-EPCs incubated in EBM-2 alone, the addition of SAL did not affect

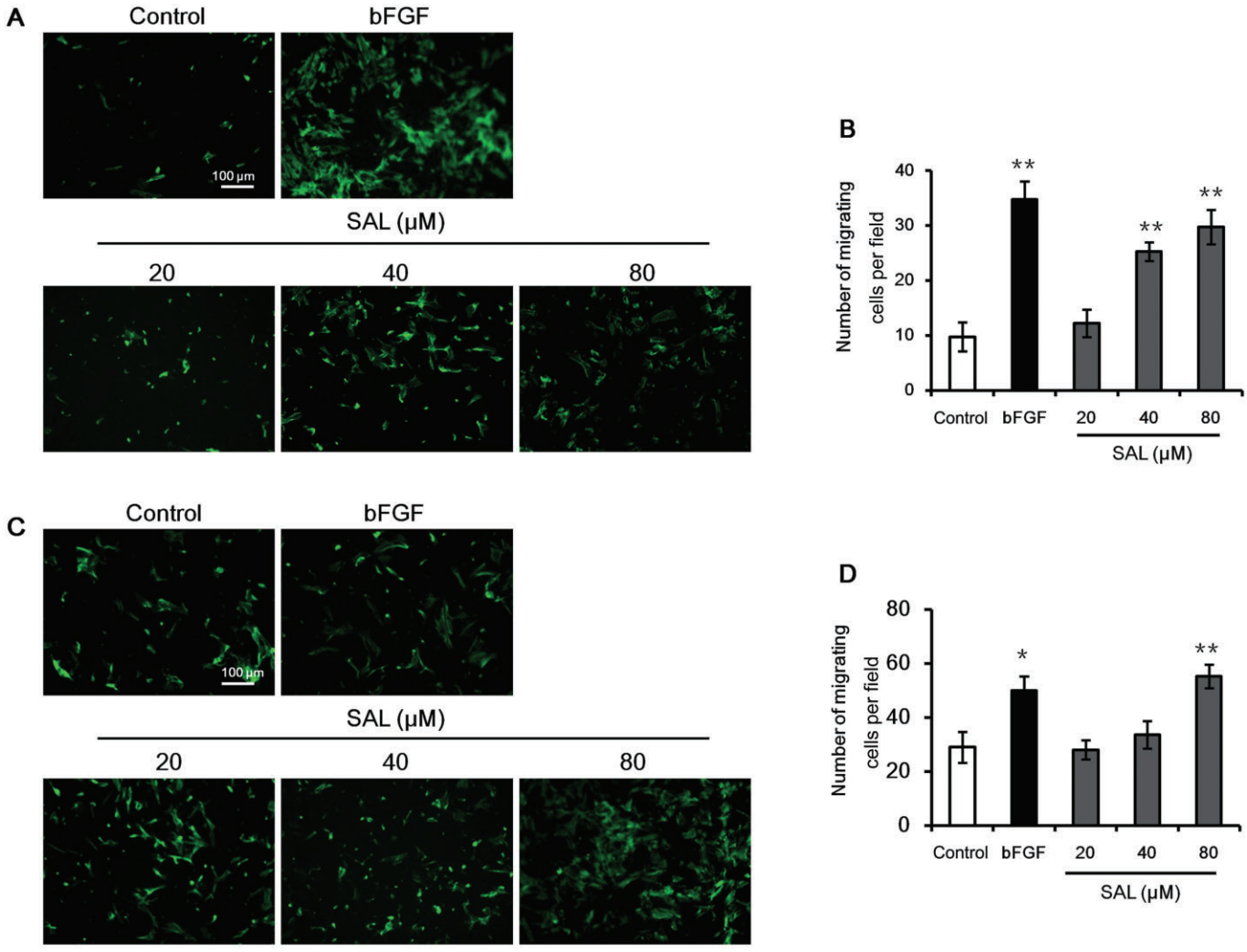

Figure 2

SAL enhances cell migration capacity in a dose-dependent manner. (A and B) Transwell chemotaxis assay was performed on BM-EPCs with PBS (control), 50 ng·mL^{-1} Bfgf, and 20, 40 and 80 μM SAL in the lower chamber. To quantify the migrated EPCs on the membrane, the upper side of the membrane was washed and wiped with a cotton swab. Transwell membranes were stained with Alexa Fluor 488 phalloidin and the migrated cells were examined using an inverted fluorescence microscopy. The number of migrated cells was quantified by performing cell counts of 10 random fields. Data are presented as mean ± SD, $n = 5$, $^{**}P < 0.01$ versus control group. (C and D) BM-EPCs were treated in the absence or presence of indicated concentrations of SAL and bFGF for 48 h, then seeded into the upper chamber of the transwell with culture medium containing 5% FBS in the lower chamber. Data are presented as mean ± SD, $n = 5$, $^{*}P < 0.05$, $^{**}P < 0.01$ versus control group.

the rate of ROS produced. After exposure to 1 mM H_2O_2 for 6 h, fluorescence microscopy revealed that intracellular ROS had accumulated significantly in EPCs as shown by an enhanced rate of intracellular dichlorofluorescin diacetate accumulation as compared with non–H_2O_2-treated control cultures (3.69 ± 0.08-fold), but pretreatment with SAL annihilated ROS production to nearly physiological levels (1.60 ± 0.15-fold at 40 μM SAL and 1.47 ± 0.13-fold at 80 μM SAL compared with non–H_2O_2-treated control) (Figure 6E). Furthermore, 48 h pretreatment with 40 and 80 μM SAL significantly decreased H_2O_2-induced NADPH production by 23.14 ± 2.32% and 29.48 ± 5.30% respectively (Figure 6F). These findings suggest that SAL has a potent antioxidant activity on H_2O_2-induced ROS production and this may be mediated at least partly through inhibition of NADPH oxidase activity. To assess the role of NADPH, diphenyliodonium (DPI), a NADPH oxidase inhibitor, was added to the cells for 90 min prior to H_2O_2 stimulation. DPI (10 μM) treatment significantly attenuated H_2O_2-induced generation of ROS (46.64 ± 4.57%) as well as reduction on cellular viability (138.11 ± 12.41%). These effects were further enhanced when combined with 80 μM SAL (Figure 6G and H).

SAL protects mitochondrial function and inhibits mitochondrion-induced apoptosis

Furthermore, the mitochondrial function of the BM-EPCs was monitored using the fluorescent dye Rhodamine 123. After incubation with H_2O_2 for 6 h, the mean fluorescence

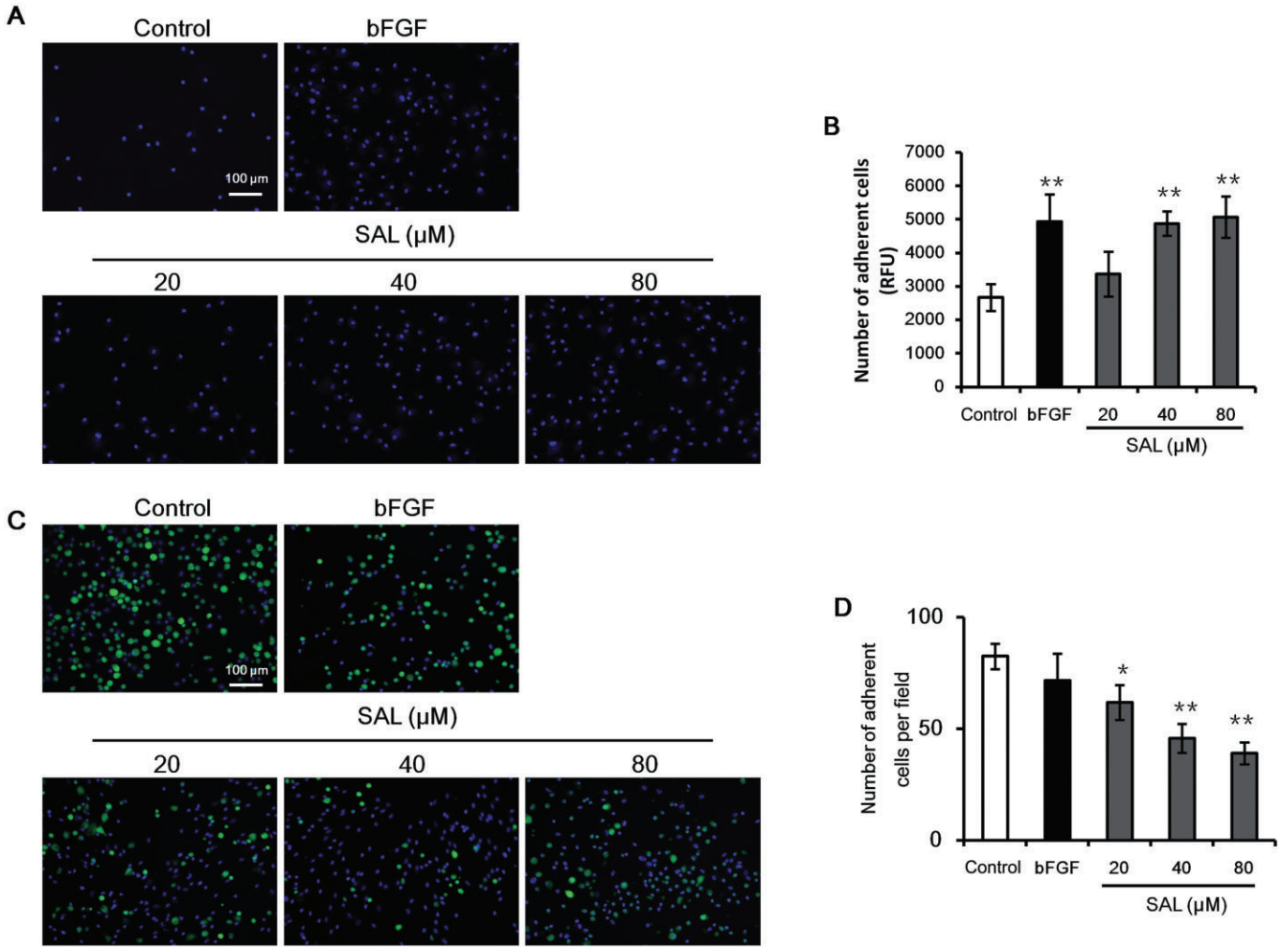

Figure 3

SAL promotes cell–matrix adhesion but inhibits cell–cell adhesion of BM-EPCs. (A) BM-EPCs were treated with 0 (control), 20, 40 and 80 μM SAL for 2 days. Cell adhesion to ECM was performed on fibronectin-treated plates for 30 min followed by staining of adherent cells with Hoechst 33258 dye (nuclei, blue). (B) Quantification of attached cells was determined by *DNA* content using Quant-iT PicoGreen ds*DNA* Assay Kit. Data are presented as mean ± SD, $n = 5$, $^{*}P < 0.05$, $^{**}P < 0.01$ versus control group. (C and D) BM-EPCs were grown overnight to a confluent monolayer in Endothelial Cell Growth Medium 2 and labelled with Hoechst 33258 dye. Another set of BM-EPCs was treated with 40 or 80 μM SAL for 48 h, fluorescence-labelled with calcein-AM for 1 h, and plated onto the established cell monolayer. Quantification of cell–cell adhesion was performed by counting the number of cells per microscopic field of view that remained attached after 20 min incubation. Data are presented as mean ± SD, $n = 5$, $^{*}P < 0.05$, $^{**}P < 0.01$ versus control group.

intensity decreased to 65.5% compared with control cells (Figure 7A and B) corresponding to a loss of MMP and to mitochondrial oxidation. SAL at 40 and 80 μM alleviated mitochondrial injury by increasing the fluorescence intensity to 90.1 and 99.2%, respectively, thereby restoring the potential to almost physiological levels (Figure 7B). Moreover, cells exposed to H_2O_2 exhibited enhanced DHE fluorescence when compared with control cells (Figure 7C). However, the H_2O_2 mediated increase in DHE fluorescence was entirely prevented by co-administration of SAL (Figure 7A and C). This implies a suppressive effect of ROS production by SAL. Furthermore, annexin V-FITC and PI double staining was employed to investigate the effect of SAL on H_2O_2-induced apoptosis. As shown in Figure 7D, the apoptosis and necrosis rates were significantly decreased after cells were treated with both 40 and 80 μM SAL for 48 h.

SAL induces angiogenic differentiation via Akt/mTOR/p70S6K and ERK1/2 pathways

To determine the underlying mechanism involved in the proangiogenic effects of SAL, the expression of VEGF, VEGFR2, VE-cadherin, vWF, PECAM-1 and eNOS were determined by quantitative RT-PCR. As shown in Figure 8A, the expression levels of VEGF, VEGFR2 and eNOS significantly increased after 2 days (1.46 ± 0.24-fold, 1.96 ± 0.20-fold, 2.82 ± 0.37-fold) and 10 days (1.61 ± 0.15-fold, 1.66 ± 0.22-fold, 3.18 ± 0.42-fold) pretreatment with SAL. While vWF gene

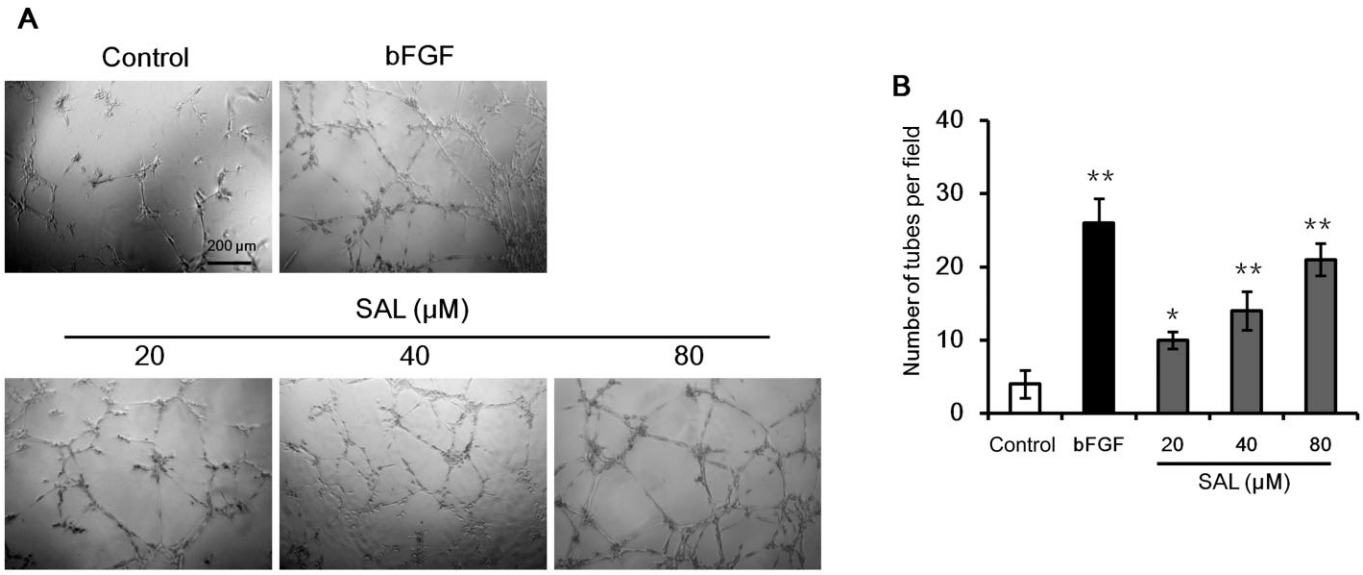

Figure 4

Effect of SAL on capillary tube formation in BM-EPCs. (A) After SAL treatment cells were grown on Matrigel™ for 18 h under normal growth conditions, capillary tube formation was observed by inverted light microscopy. (B) Five independent fields were assessed for each well and the average numbers of tubes per 40× magnified field were determined. Data are expressed as mean ± SD, $n = 5$, *$P < 0.05$, **$P < 0.01$ versus control group.

expression was enhanced after 2 days (1.79 ± 0.22-fold) and 10 days (2.20 ± 0.29-fold) cultivation, PECAM-1 expression was increased only after 2 days (2.01 ± 0.18-fold) cultivation (Figure 8A). VE-cadherin expression was down-regulated by 67.8% after 2 days and by 78.0% after 10 days with a similar trend for bFGF expression (Figure 8A).

Evaluating key pathway components involved in cellular function and angiogenesis, we found that SAL effectively triggered the phosphorylation of mTOR signalling cascade, including Akt, mTOR and p70S6K kinase (ser 371) in BM-EPCs in a concentration-dependent manner (Figure 8B). Furthermore, we used the highly specific PI3K inhibitor LY294002 to assess the role of the PI3K/Akt pathway in angiogenesis. Unexpectedly, LY294002 inhibited not only Akt, but also notably phosphorylated mTOR (Figure 8C). Cell migration and tube formation ability were significantly decreased when SAL was co-administered with LY294002 (Figure 8E and F), suggesting that SAL promotes cell mobility and angiogenesis through activating the Akt/mTOR signalling pathway. To further define the roles of MAPK in the SAL-induced effects on BM-EPCs, we analysed the expression of phosphorylated ERK1/2, p38 MAPK and JNK following SAL treatment. As demonstrated in Figure 8B, the phosphorylation levels of ERK1/2 were increased after SAL treatment for 48 h. However, no significant changes of phosphorylation levels of p38 MAPK and JNK were observed after SAL treatment (data not shown). Additionally, application of ERK1/2 inhibitor U0126 also markedly reduced the phosphorylated expression of mTOR (Figure 8D) and blocked SAL-induced cell migration as well as angiogenesis (Figure 8E and F). This implies that, by interaction with mTOR, ERK1/2 is a potential target of SAL in BM-EPCs.

SAL prevents H_2O_2-induced cell injury via JNK, p38 MAPK pathways and modulates Bcl-2 family protein expression

In order to investigate the mechanisms underlying the cytoprotective effects of SAL in relation to oxidative stress, the expression of Nox4, STAT-3 as well as selected endothelial marker genes were investigated. Both Nox4 and STAT-3 expression levels were considerably decreased by 59.8 and 19.8% after SAL preincubation (Figure 9A). SAL treatment recovered the H_2O_2-induced decrease in VEGF gene expression to nearly physiological levels. In addition, H_2O_2-stressed BM-EPCs preincubated with SAL showed enhanced VEGFR2 expression as compared with non–SAL-treated cells (1.78 ± 0.09-fold). Compared with untreated cells, H_2O_2-stimulated cells showed a significantly higher eNOS expression, however, pretreatment with SAL for 48 h lead to an 87% reduction of its level (Figure 9A).

As Bcl-2 family proteins are crucial players in apoptosis by functioning as promoters or inhibitors of cell death processes we studied the changes in the levels of Bax/Bcl-xL in BM-EPCs upon H_2O_2 exposure. Western blot analysis showed that 1 mM H_2O_2 caused a profound up-regulation of the pro-apoptotic protein Bax and a down-regulation of anti-apoptotic proteins Bcl-xL. SAL preincubation reversed the increased Bax/Bcl-xL ratio by declining Bax and restoring Bcl-xL expression (Figure 9B and D). To further elucidate the underlying mechanisms of the SAL-mediated cytoprotective effects in a pathway-orientated manner, phosphorylation rates of JNK, p38 MAPK, and ERK1/2 in H_2O_2-stressed BM-EPCs were determined in relation to SAL treatment. As shown in Figure 9B, stimulation of BM-EPCs with H_2O_2-

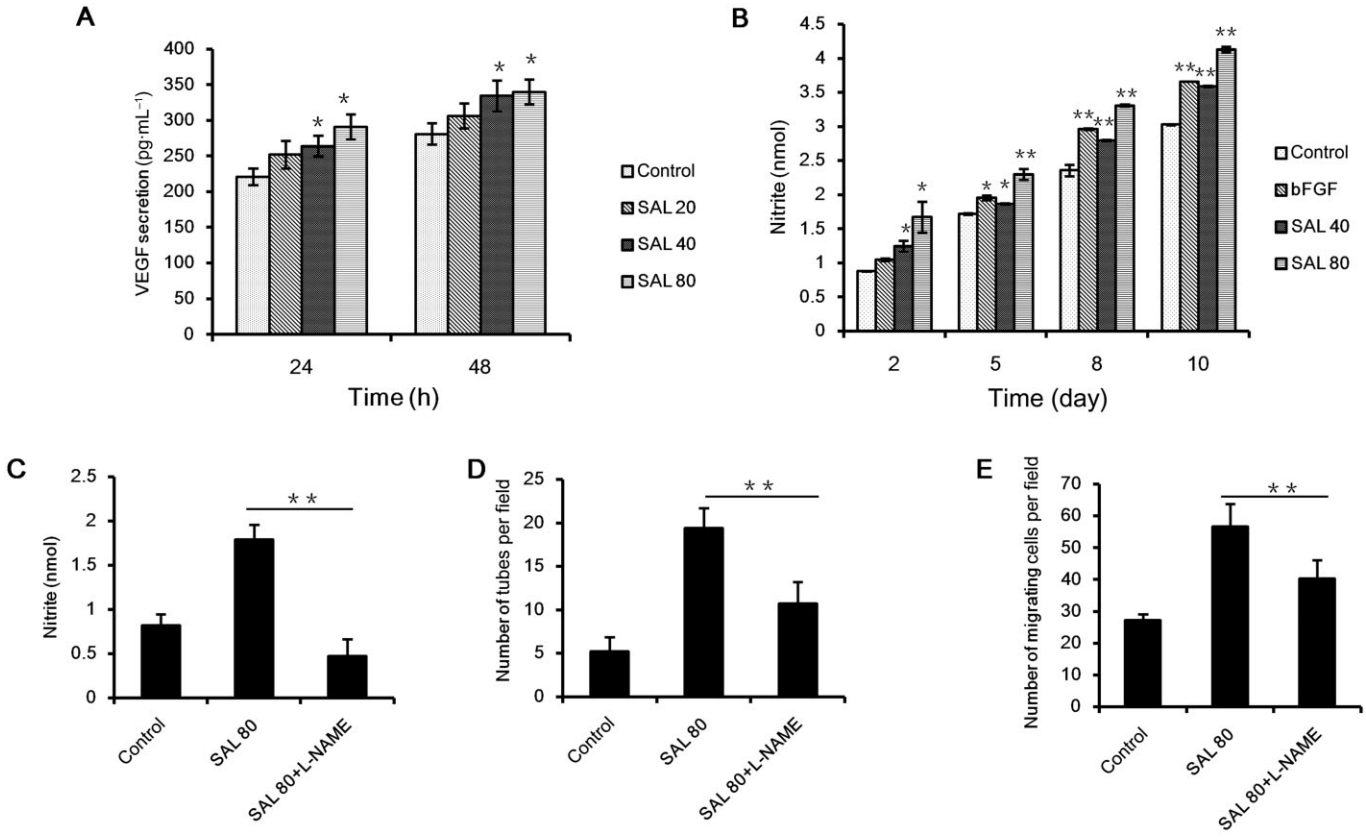

Figure 5

SAL enhances the secretion of VEGF and the production of NO in BM-EPCs. Cells were cultured until confluency in 96-well plates and subsequently stimulated with 0 (control), 20, 40 and 80 μM SAL. (A) Cell culture supernatants were collected after 24 and 48 h and VEGF secretion was determined by ELISA, $n = 5$. (B) To assess NO production, cell culture supernatants were collected 2, 5, 8 and 10 days after SAL stimulation and analysed by Griess assay, $n = 4$. (C) Cell culture supernatants were collected 48 h after SAL stimulation with or without 10 μM L-NAME, NO levels were measured by Griess assay, $n = 3$. (D and E) BM-EPCs were treated with 10 μM L-NAME and 80 μM SAL for 48 h. Cell migratory ability was evaluated by performing cell counts in 10 random fields. Capillary-like tube formation were determined by assessing average numbers of tubes per 40× magnified field, $n = 3$. All data are presented as mean ± SD, $^*P < 0.05$, $^{**}P < 0.01$ versus control group.

induced phosphorylation of all the three target proteins, whereas SAL pretreatment significantly inhibited the up-regulation of both phosphorylated JNK and p38 MAPK, but not ERK1/2 (Figure 9B and C).

Discussion

In vitro tissue vascularization is an upcoming strategy to solve the problem of insufficient blood supply upon construct implantation. Although recent publications show promising results, these studies were generally performed with endothelial cell model systems not enabling translational conclusions (Verseijden *et al.*, 2010; 2012). Primary cells, however, are valuable tools enabling the study of a variety of cellular and biochemical functions under tightly controlled experimental conditions. To effectively facilitate the treatment of diseases caused by ischemia, there is a need for developing safe and cost-effective proangiogenic drugs. In the present study, we used human primary BM-EPCs cultivated with EGM-2 at passages 3–5 that can be categorized as late-outgrowth EPC to demonstrate the effects of SAL on cellular proliferation and differentiation and the underlying subcellular mechanisms. We found that SAL acts on BM-EPCs by promoting cellular proliferation, as well as enhancing key functional activities including migration, cell–matrix adhesion and tube formation. Moreover, on the one hand, SAL significantly increased VEGF secretion and NO production by BM-EPCs, and on the other hand exerted a considerable cytoprotective effect in relation to oxidative stress.

Previous studies have demonstrated that the value of the 50% effective concentration (EC_{50}) of SAL on tacrine-induced cytotoxicity in Hep G2 cells was 51.3 μM (Song *et al.*, 2003), and that SAL at 33 μM significantly reduced apoptosis in response to cobalt chloride (Tan *et al.*, 2009). Based on these reports, we decided to use SAL at concentrations ranging from 10 to 80 μM.

Angiogenesis is a complex process requiring multiple sequential steps including interplay between cells, soluble factors and ECM components. Vascular endothelium proliferation is the first step in angiogenesis, including processes like migration, differentiation, survival and death. Under the

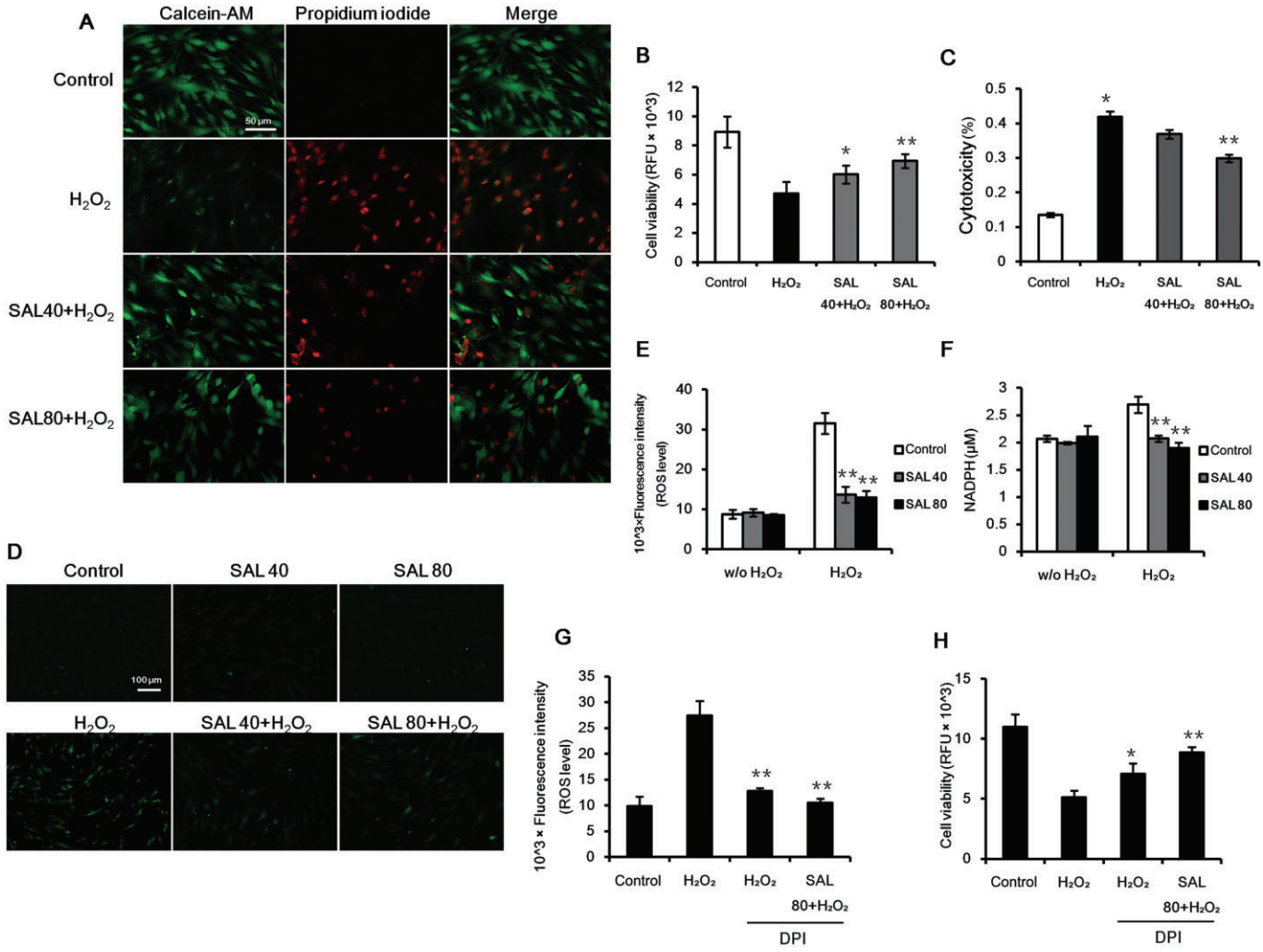

Figure 6

SAL protects BM-EPCs from H_2O_2-induced cell damage and ROS production. (A) Cells were pretreated with 0 (control), 40, 80 μM SAL and stressed by 1 mM H_2O_2. Cell survival was monitored by calcein AM/PI double staining and analysed qualitatively by fluorescence microscopy. Representative micrographs from each treatment group are shown. (B) After the treatment with SAL and induction by 1 mM H_2O_2, BM-EPCs were washed with PBS and cellular viability was evaluated by quantification of *DNA* content, $n = 6$. (C) Cell death was evaluated by LDH assay, $n = 4$. (D) Cells were pretreated with 40 and 80 μM SAL for 48 h, labelled with 30 μM DCFH-DA and subsequently stressed with H_2O_2 for 6 h prior to fluorescence microscopy. (E) Production of ROS was quantified by the amount of DCF formed in the BM-EPCs. The fluorescence intensity was measured using a microplate reader, $n = 6$. (F) Cells were treated with 40 and 80 μM SAL for 48 h, followed by H_2O_2 treatment for 6 h. NADPH oxidase activity was measured colourimetrically using NADP/NADPH assay kit, $n = 5$. (G and H) Cells were treated with 80 μM SAL for 48 h, and then stimulated with H_2O_2 for 6 h after pretreatment with 10 μM DPI. ROS was quantified by DCF formation as described earlier ($n = 4$), and cellular viability was evaluated by quantification of *DNA* content ($n = 3$). All data are expressed as mean ± SD. $^*P < 0.05$, $^{**}P < 0.01$ versus H_2O_2 group.

conditions used in the present study, SAL significantly, yet non-dose-dependently, promoted proliferation of BM-EPCs at 20, 40 and 80 μM. A possible explanation for this finding may be a saturation of the cell receptors involved in cell proliferation by SAL at concentrations exceeding 20 μM. Furthermore, the absence of a time-dependent effect of SAL on EPC proliferation at the early time point of 24 h cultivation can be explained as follows. Firstly, the effect of SAL on cell proliferation is indirect via activation of the secretion of cytokines and may therefore be associated with a time delay. Secondly, the cells are metabolically more active and thus more responsive to the drug after 48 h adherence to the tissue culture polystyrene plate. Thirdly, as we used serum-free medium for the proliferation assay to reduce any potential bias on cellular function exerted by growth factors, cells grew slowly and thus the time window for observing potential proliferative effects by SAL may have been extended. The lack of an observed proliferative effect on EPC by SAL at 96 h can be at least partly explained by a reduced drug efficacy over time because of a comparatively short half-life of SAL as known from *in vivo* studies.

Homing and incorporation of EPCs to the sites of revascularization probably are determined not only by the number of circulating EPCs, but also by the motility of the cells. The

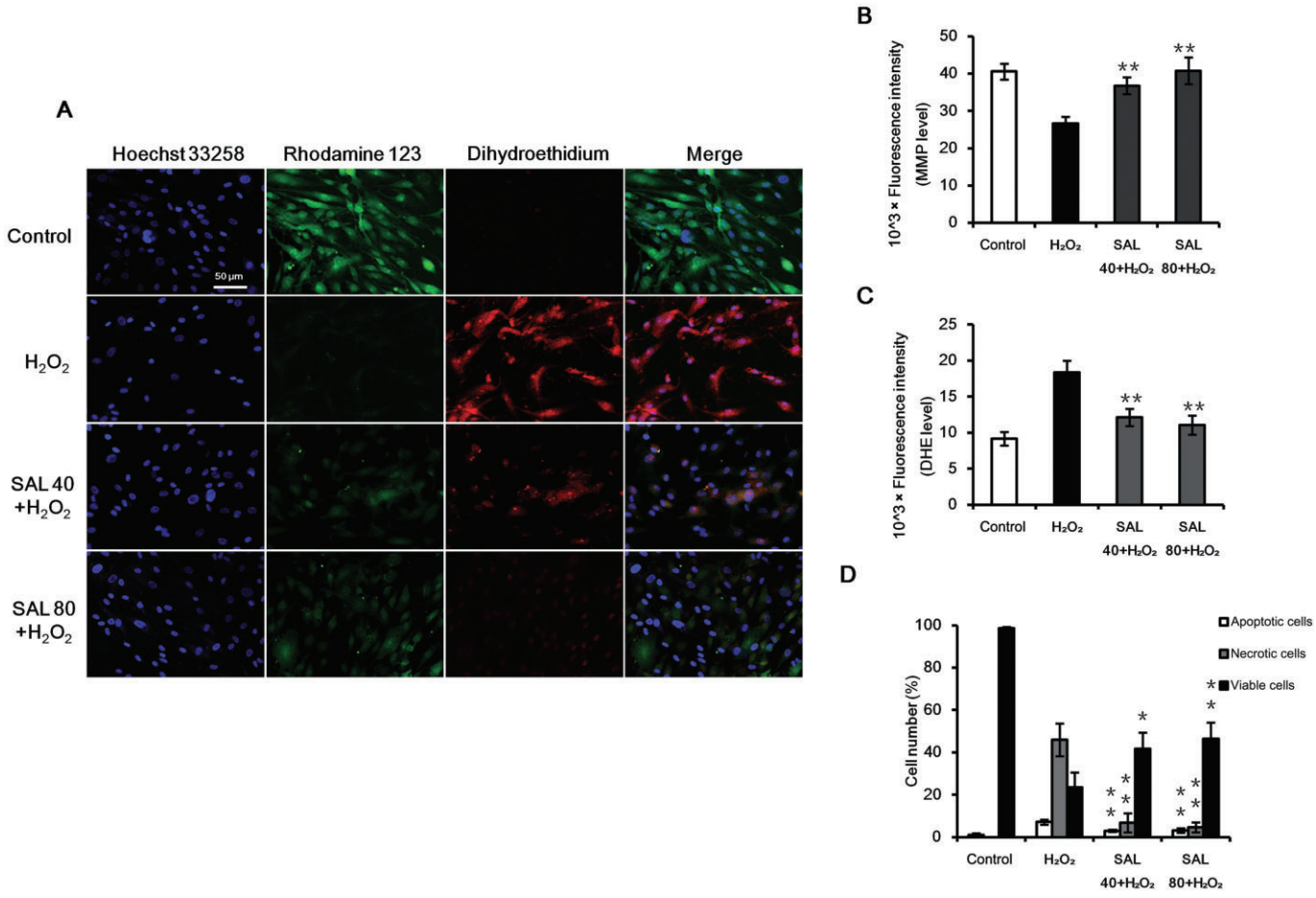

Figure 7

SAL inhibits H_2O_2-induced cell apoptosis. BM-EPCs were pretreated with 0 (control), 40, 80 μM SAL for 48 h and stressed by 1 mM H_2O_2. (A) Then cells were labelled with the fluorescent dye Rhodamine 123, the superoxide indicator DHE and the nucleic acid stain Hoechst 33258, $n = 4$. (B) BM-EPCs were loaded with 5 μM Rhodamine 123. After 20 min incubation in the dark, cells were washed twice with PBS, and the plates were immediately read using a fluorescent plate reader, $n = 5$. (C) Cells were probed with 10 μM DHE for 30 min, fluorescence intensity was determined using a fluorescent plate reader, $n = 4$. (D) Cells were harvested and labelled with a combination of annexin V-FITC and PI. H_2O_2-induced apoptosis was determined by flow cytometry, $n = 3$. All data are expressed as mean ± SD. $^*P < 0.05$, $^{**}P < 0.01$ versus H_2O_2 group.

present study provides evidence that SAL not only increases the chemotactic response of BM-EPC but SAL can trigger the cells' innate chemoattractive potency, *per se*.

VEGF is one of the most potent angiogenic cytokines and promotes proliferation of vascular cells. Interestingly, there are several reports describing that VEGF increases vascular permeability and endothelial cell survival in quiescent vessels, and the cellular responses to these effectors involve disruption of the VE-cadherin-based adherent junction (Gavard and Gutkind, 2006; Mura *et al.*, 2006; Wong *et al.*, 2009). In our study, SAL stimulated EPCs tubule formation *in vitro* accompanied by enhanced mRNA expression and protein secretion of VEGF. Additionally, the mRNA expression of eNOS, vWF and PECAM1 were up-regulated by SAL. Furthermore, we observed that SAL regulated EPC mobilization and differentiation via up-regulation of VEGF and its receptor VEGFR2. VE-cadherin is a transmembrane or membrane-associated glycoprotein that mediates specific cell–cell adhesion in a Ca^{2+}-dependent manner (Egami *et al.*, 2005; Montero-Balaguer *et al.*, 2009). VE-cadherin knockdown in HUVEC resulted in increased tubule formation indicating that it is loss of VE-cadherin that leads to increased angiogenesis (Mavria *et al.*, 2006). In the present study, the low expression of VE-cadherin after SAL treatment suggests decreased cell–cell adhesion that may contribute to the enhanced angiogenic effect exerted by SAL.

The role of NO as a major regulator of cell migration and angiogenesis is suggested by the observation that it is produced by eNOS following its activation downstream of the VEGFR-2/PI3K/Akt (PKB) axis in endothelial cells activated by VEGF (Williams *et al.*, 2000). Endothelial-derived NO is essential for the maintenance of vascular homeostasis (Drummond *et al.*, 2000; Matz *et al.*, 2000; Murohara and Asahara, 2002). Our results reveal a continuously increasing production of NO over time exerted by SAL treatment. However, inhibition of NOS by L-NAME considerably attenuated the promotion effect of SAL on cell migration and tubular formation, implying that NO essentially participates in the angiogenic events.

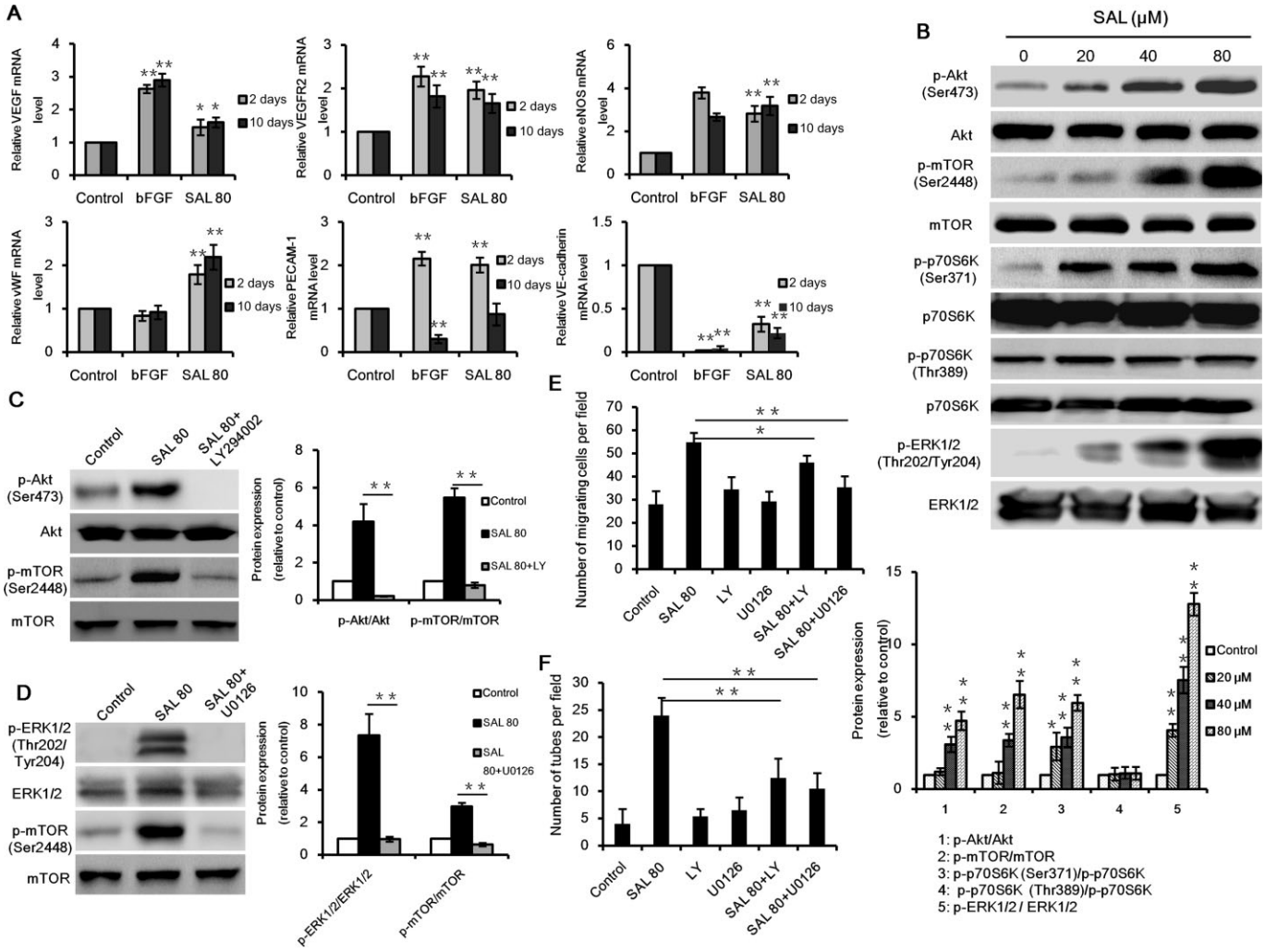

Figure 8

Gene expression and signal pathway analysis of SAL-treated BM-EPCs. (A) BM-EPCs were cultivated in endothelial basal medium with or without 80 μM SAL for 2 and 10 days. Gene expression levels of VEGF, VEGFR2, eNOS, VE-cadherin, vWF and PECAM-1 were assessed via quantitative real-time PCR. Data were normalized to GAPDH expression and fold changes were calculated by the $2^{-\Delta\Delta CT}$ method; $n = 5$, $^{*}P < 0.05$, $^{**}P < 0.01$ versus control group. (B) BM-EPCs were treated with 0 (control), 20, 40 and 80 μM SAL for 48 h and then harvested. Total cell lysates were prepared and subjected to SDS-PAGE, followed by Western blot analysis. The immunoblots shown are representative of at least three independent experiments with comparable results. Densitometric analysis was done using Quantity One software and shown in the lower panel. $^{*}P < 0.05$, $^{**}P < 0.01$ versus control group. (C and D) BM-EPCs were pretreated with either 20 μM LY294002 or 10 μM U0126 for 90 min, then cultured with 0 (control) or 80 μM SAL for 48 h. Protein expression was analysed by Western blot analysis. Densitometric analyses of band intensities normalized to the total proteins or GAPDH are shown in the right panels, $n = 5$. $^{**}P < 0.01$ versus SAL 80 group. (E and F) BM-EPCs were treated under the same conditions described earlier, cell migratory ability and capillary-like tube formation were determined as described above, $n = 3$. $^{*}P < 0.05$, $^{**}P < 0.01$ versus SAL 80 group. All data are presented as mean ± SD.

We furthermore investigated the effects of SAL on the Akt/mTOR/p70S6K and MAPK pathways. Recently, several studies have shown the role of p70S6K, a direct downstream target of mTORC1 (mTOR, GβL and raptor) in modulating cell migration (Berven *et al.*, 2004; Qiu *et al.*, 2004). Of note, it seems that the primary pathway by which most growth factors and cytokines activate mTOR and its downstream targets is the PI3K/Akt (Li *et al.*, 1999; Fingar and Blenis, 2004). MAPK signalling is critical during the endothelial differentiation of vascular progenitor cell (Takahashi *et al.*, 2012). In our study, treatment with SAL showed a marked increase in the phosphorylation of mTOR, p70S6K and its upstream kinase Akt. Moreover, the phosphorylation level of ERK1/2 was increased significantly upon SAL stimulation. In further blocking experiments we observed that LY294002 and U0126 significantly inhibited phosphorylated Akt and ERK1/2 and phosphorylated mTOR and consequently led to a decrease in cell migration and tube formation capacity in BM-EPCs. These data suggest that SAL promotes proliferation and differentiation of EPCs and enhances their functions via activation of the Akt/mTOR/p70S6K and ERK1/2 pathways.

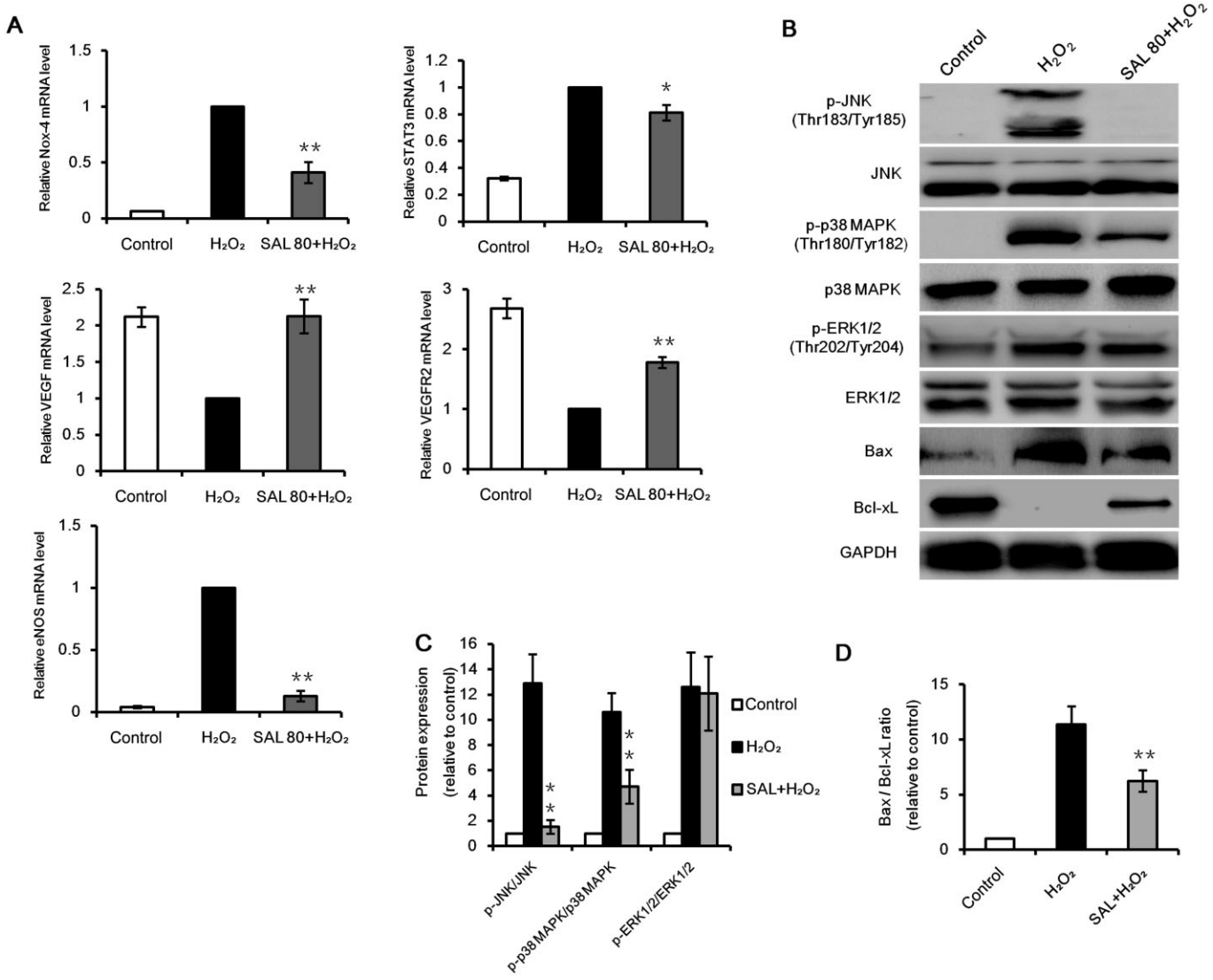

Figure 9

Gene expression and signal pathway analysis of H_2O_2-treated BM-EPCs. (A) BM-EPCs were treated with 80 μM SAL for 2 days, then incubated with 1 mM H_2O_2 for 6 h and gene expression levels of Nox4, STAT3, VEGF, VEGFR2, eNOS were determined, $n = 3$. (B) Cells were incubated without or with 80 μM SAL for 48 h before stimulation with 1 mM H_2O_2. Total protein (30 μg) was isolated from the cells, applied to Western blotting and probed with specific antibodies. The immunoblots shown here are representative of at least three independent experiments with similar results. (C and D) Densitometric analyses of band intensities normalized to the total proteins or GAPDH are shown. All data are presented as mean ± SD. *$P < 0.05$, **$P < 0.01$ versus H_2O_2 group.

Another new finding of the present study is that H_2O_2-induced cytotoxicity is counteracted by SAL. Usually the imbalance caused by oxidative stress is derived either from an increase in ROS production or from a decreased level of ROS scavenging proteins. Here, H_2O_2-induced oxidative stress was found to be dependent on a significant production of ROS in EPCs, which in turn was associated with an up-regulation of Nox4, STAT-3 and eNOS. SAL significantly increased cell viability and declined cell death in EPCs subjected to H_2O_2-induced oxidative stress by reducing ROS formation and attenuating the increased expression of Nox4, STAT-3 and eNOS. NADPH oxidase is one of the most prominent sources of vascular ROS, which is expressed in a variety of vascular cells. The importance of NADPH oxidase in both vascular physiology and pathophysiology has been emphasized extensively (Li and Shah, 2003; Frey *et al.*, 2009). Nox4 is abundantly expressed in endothelial cells and functions as a key endothelial NADPH oxidase membrane component (Ago *et al.*, 2004). In this regard, the present data show that SAL attenuates the up-regulation of NADPH oxidase and Nox4 expression, as well as DPI-abolished NADPH oxidase-mediated ROS formation. This suggests that the inhibition of ROS production and the subsequent protective effect of SAL against oxidation are likely to be related to the suppression of

NADPH oxidase. Furthermore, cell apoptosis was suppressed by SAL after H_2O_2 provocation, which was evidenced by preventing the loss of MMP and maintaining the integrity of the plasma membrane.

Members of the Bcl-2 family of proteins have a central role in controlling the apoptotic pathway. Some proteins within this family, including Bcl-2 and Bcl-xL, suppress apoptosis, while others such as Bax and Bak promote apoptosis. Hence, alterations in the levels of anti- and pro-apoptotic Bcl-2 family proteins are critical for the induction of apoptosis. We found that H_2O_2 stress resulted in an increased expression of Bax protein and a decreased expression of Bcl-xL. Pretreatment with SAL reversed this effect thereby decreasing the Bax/Bcl-xL ratio. Therefore, it is conclusive to postulate that down-regulation of Bax and up-regulation of Bcl-xL may be responsible for the observed anti-apoptotic effect of SAL. Furthermore, SAL also attenuated the up-regulation of both phosphorylated JNK and p38 MAPK induced by H_2O_2, implying a possible role of JNK and p38 MAPK in the cytoprotective potency of SAL. Xu and co-workers found that SAL is capable of protecting HUVECs against H_2O_2-induced apoptosis by inhibiting ROS production and by activating the PI3K/Akt/mTOR-dependent pathway (Xu *et al.*, 2013). Dai *et al.* observed that the reduction of oxidative stress enhances endothelial cell survival thereby facilitating ischaemia-mediated angiogenesis (Dai *et al.*, 2009). Taken together, it is likely that the antioxidative effect of SAL contributes to an increased angiogenic ability in BM-EPCs.

Limitations of the present study include the lack of preclinical *in vivo* data as well as gene knockdown experiments to further evaluate the role of angiogenic marker genes, for example eNOS, VEGF and vWF in the context of SAL-mediated EPC stimulation.

In conclusion, the present study demonstrates that SAL induces proliferation and enhances migration, cell–matrix adhesion, and capillary structure formation in BM-EPCs. In addition, SAL attenuates the cytotoxic and pro-apoptotic effect of H_2O_2 *in vitro*. The present results provide mechanistic evidence that the pro-proliferative and pro-angiogenic effects of SAL are associated with regulation of the Akt/mTOR/p70S6K and MAPK/ERK1/2 signalling pathways. The anti-apoptotic effect exerted by SAL is mediated by the inactivation of phosphorylated JNK and p38 MAPK, and a decreased Bax/Bcl-xL expression ratio. Based on the outcomes of the present study we propose SAL as a novel pro-anigiogenic therapeutic agent with potential applications in the fields of systemic and site-specific tissue regeneration including ischaemic disease and extended musculoskeletal tissue defects.

Acknowledgements

The authors wish to express their gratitude to Prof. Dr. Martin Bornhäuser, Dr. Manja Wobus and Katrin Müller for providing bone marrow samples. This study was supported by the German Academic Exchange Service and Federal Ministry of Education and Research (D/09/04774), and Chinese National Program on Key Basic Research (973 Program, No. 2012CB619100).

Conflict of interest

None.

References

Ago T, Kitazono T, Ooboshi H, Iyama T, Han YH, Takada J *et al.* (2004). Nox4 as the major catalytic component of an endothelial NAD(P)H oxidase. Circulation 109: 227–233.

Alexander SPH, Benson HE, Faccenda E, Pawson AJ, Sharman JL, Spedding M, Peters JA, Harmar AJ and CGTP Collaborators (2013). The Concise Guide to PHARMACOLOGY 2013/14: Catalytic Receptors. Br J Pharmacol 170: 1676–1705.

Asahara T, Kawamoto A (2004). Endothelial progenitor cells for postnatal vasculogenesis. Am J Physiol Cell Physiol 287: C572–C579.

Asahara T, Murohara T, Sullivan A, Silver M, van der Zee R, Li T *et al.* (1997). Isolation of putative progenitor endothelial cells for angiogenesis. Science 275: 964–967.

Atesok K, Li R, Stewart DJ, Schemitsch EH (2010). Endothelial progenitor cells promote fracture healing in a segmental bone defect model. J Orthop Res 28: 1007–1014.

Berven LA, Willard FS, Crouch MF (2004). Role of the p70(S6K) pathway in regulating the actin cytoskeleton and cell migration. Exp Cell Res 296: 183–195.

Dai S, He Y, Zhang H, Yu L, Wan T, Xu Z *et al.* (2009). Endothelial-specific expression of mitochondrial thioredoxin promotes ischemia-mediated arteriogenesis and angiogenesis. Arterioscler Thromb Vasc Biol 29: 495–502.

Darbinyan V, Kteyan A, Panossian A, Gabrielian E, Wikman G, Wagner H (2000). Rhodiola rosea in stress induced fatigue – a double blind cross-over study of a standardized extract SHR-5 with a repeated low-dose regimen on the mental performance of healthy physicians during night duty. Phytomedicine 7: 365–371.

De Bock K, Eijnde BO, Ramaekers M, Hespel P (2004). Acute Rhodiola rosea intake can improve endurance exercise performance. Int J Sport Nutr Exerc Metab 14: 298–307.

De Vriese AS, Verbeuren TJ, Van de Voorde J, Lameire NH, Vanhoutte PM (2000). Endothelial dysfunction in diabetes. Br J Pharmacol 130: 963–974.

Dimmeler S, Zeiher AM (2004). Vascular repair by circulating endothelial progenitor cells: the missing link in atherosclerosis? J Mol Med 82: 671–677.

Drummond GR, Cai H, Davis ME, Ramasamy S, Harrison DG (2000). Transcriptional and posttranscriptional regulation of endothelial nitric oxide synthase expression by hydrogen peroxide. Circ Res 86: 347–354.

Egami R, Tanaka Y, Nozaki M, Koera K, Okuma A, Nakano H (2005). Chronic treatment with 17beta-estradiol increases susceptibility of smooth muscle cells to nitric oxide. Eur J Pharmacol 520: 142–149.

Fingar DC, Blenis J (2004). Target of rapamycin (TOR): an integrator of nutrient and growth factor signals and coordinator of cell growth and cell cycle progression. Oncogene 23: 3151–3171.

Frey RS, Ushio-Fukai M, Malik AB (2009). NADPH oxidase-dependent signaling in endothelial cells: role in physiology and pathophysiology. Antioxid Redox Signal 11: 791–810.

Gavard J, Gutkind JS (2006). VEGF controls endothelial-cell permeability by promoting the beta-arrestin-dependent endocytosis of VE-cadherin. Nat Cell Biol 8: 1223–1234.

Gunsilius E, Duba HC, Petzer AL, Kahler CM, Grunewald K, Stockhammer G *et al*. (2000). Evidence from a leukaemia model for maintenance of vascular endothelium by bone-marrow-derived endothelial cells. Lancet 355: 1688–1691.

Hoetzer GL, Van Guilder GP, Irmiger HM, Keith RS, Stauffer BL, DeSouza CA (2007). Aging, exercise, and endothelial progenitor cell clonogenic and migratory capacity in men. J Appl Physiol 102: 847–852.

Iwakura A, Luedemann C, Shastry S, Hanley A, Kearney M, Aikawa R *et al*. (2003). Estrogen-mediated, endothelial nitric oxide synthase-dependent mobilization of bone marrow-derived endothelial progenitor cells contributes to reendothelialization after arterial injury. Circulation 108: 3115–3121.

Iwakura A, Shastry S, Luedemann C, Hamada H, Kawamoto A, Kishore R *et al*. (2006). Estradiol enhances recovery after myocardial infarction by augmenting incorporation of bone marrow-derived endothelial progenitor cells into sites of ischemia-induced neovascularization via endothelial nitric oxide synthase-mediated activation of matrix metalloproteinase-9. Circulation 113: 1605–1614.

Kalka C, Masuda H, Takahashi T, Kalka-Moll WM, Silver M, Kearney M *et al*. (2000). Transplantation of ex vivo expanded endothelial progenitor cells for therapeutic neovascularization. Proc Natl Acad Sci U S A 97: 3422–3427.

Kawamoto A, Asahara T, Losordo DW (2002). Transplantation of endothelial progenitor cells for therapeutic neovascularization. Cardiovasc Radiat Med 3: 221–225.

Kushner EJ, Van Guilder GP, Maceneaney OJ, Cech JN, Stauffer BL, DeSouza CA (2009). Aging and endothelial progenitor cell telomere length in healthy men. Clin Chem Lab Med 47: 47–50.

Li J, DeFea K, Roth RA (1999). Modulation of insulin receptor substrate-1 tyrosine phosphorylation by an Akt/phosphatidylinositol 3-kinase pathway. J Biol Chem 274: 9351–9356.

Li JM, Shah AM (2003). Mechanism of endothelial cell NADPH oxidase activation by angiotensin II. Role of the p47phox subunit. J Biol Chem 278: 12094–12100.

Maslov LN, Lishmanov YB, Arbuzov AG, Krylatov AV, Budankova EV, Konkovskaya YN *et al*. (2009). Antiarrhythmic activity of phytoadaptogens in short-term ischemia-reperfusion of the heart and postinfarction cardiosclerosis. Bull Exp Biol Med 147: 331–334.

Matz RL, de Sotomayor MA, Schott C, Stoclet JC, Andriantsitohaina R (2000). Vascular bed heterogeneity in age-related endothelial dysfunction with respect to NO and eicosanoids. Br J Pharmacol 131: 303–311.

Mavria G, Vercoulen Y, Yeo M, Paterson H, Karasarides M, Marais R *et al*. (2006). ERK-MAPK signaling opposes Rho-kinase to promote endothelial cell survival and sprouting during angiogenesis. Cancer Cell 9: 33–44.

Montero-Balaguer M, Swirsding K, Orsenigo F, Cotelli F, Mione M, Dejana E (2009). Stable vascular connections and remodeling require full expression of VE-cadherin in zebrafish embryos. PLoS ONE 4: e5772.

Mura M, Han B, Andrade CF, Seth R, Hwang D, Waddell TK *et al*. (2006). The early responses of VEGF and its receptors during acute lung injury: implication of VEGF in alveolar epithelial cell survival. Critical care 10: R130.

Murohara T, Asahara T (2002). Nitric oxide and angiogenesis in cardiovascular disease. Antioxid Redox Signal 4: 825–831.

Palladino M, Gatto I, Neri V, Stigliano E, Smith RC, Pola E *et al*. (2012). Combined therapy with sonic hedgehog gene transfer and bone marrow-derived endothelial progenitor cells enhances angiogenesis and myogenesis in the ischemic skeletal muscle. J Vasc Res 49: 425–431.

Qiu Q, Yang M, Tsang BK, Gruslin A (2004). Both mitogen-activated protein kinase and phosphatidylinositol 3-kinase signalling are required in epidermal growth factor-induced human trophoblast migration. Mol Hum Reprod 10: 677–684.

Qu ZQ, Zhou Y, Zeng YS, Lin YK, Li Y, Zhong ZQ *et al*. (2012). Protective effects of a Rhodiola crenulata extract and salidroside on hippocampal neurogenesis against streptozotocin-induced neural injury in the rat. PLoS ONE 7: e29641.

Rozen N, Bick T, Bajayo A, Shamian B, Schrift-Tzadok M, Gabet Y *et al*. (2009). Transplanted blood-derived endothelial progenitor cells (EPC) enhance bridging of sheep tibia critical size defects. Bone 45: 918–924.

Scheubel RJ, Zorn H, Silber RE, Kuss O, Morawietz H, Holtz J *et al*. (2003). Age-dependent depression in circulating endothelial progenitor cells in patients undergoing coronary artery bypass grafting. J Am Coll Cardiol 42: 2073–2080.

Shevtsov VA, Zholus BI, Shervarly VI, Vol'skij VB, Korovin YP, Khristich MP *et al*. (2003). A randomized trial of two different doses of a SHR-5 Rhodiola rosea extract versus placebo and control of capacity for mental work. Phytomedicine 10: 95–105.

Shi Q, Rafii S, Wu MH, Wijelath ES, Yu C, Ishida A *et al*. (1998). Evidence for circulating bone marrow-derived endothelial cells. Blood 92: 362–367.

Shi TY, Feng SF, Xing JH, Wu YM, Li XQ, Zhang N *et al*. (2012). Neuroprotective effects of Salidroside and its analogue tyrosol galactoside against focal cerebral ischemia *in vivo* and H2O2-induced neurotoxicity *in vitro*. Neurotox Res 21: 358–367.

Shu H, Arita H, Hayashida M, Zhang L, An K, Huang W *et al*. (2010). Anti-hypersensitivity effects of Shu-jing-huo-xue-tang, a Chinese herbal medicine, in CCI-neuropathic rats. J Ethnopharmacol 131: 464–470.

Song EK, Kim JH, Kim JS, Cho H, Nan JX, Sohn DH *et al*. (2003). Hepatoprotective phenolic constituents of Rhodiola sachalinensis on tacrine-induced cytotoxicity in Hep G2 cells. Phytother Res 17: 563–565.

Spasov AA, Wikman GK, Mandrikov VB, Mironova IA, Neumoin VV (2000). A double-blind, placebo-controlled pilot study of the stimulating and adaptogenic effect of Rhodiola rosea SHR-5 extract on the fatigue of students caused by stress during an examination period with a repeated low-dose regimen. Phytomedicine 7: 85–89.

Sun L, Isaak CK, Zhou Y, Petkau JC, Karmin O, Liu Y *et al*. (2012). Salidroside and tyrosol from Rhodiola protect H9c2 cells from ischemia/reperfusion-induced apoptosis. Life Sci 91: 151–158.

Takahashi M, Okubo N, Chosa N, Takahashi N, Ibi M, Kamo M *et al*. (2012). Fibroblast growth factor-1-induced ERK1/2 signaling reciprocally regulates proliferation and smooth muscle cell differentiation of ligament-derived endothelial progenitor cell-like cells. Int J Mol Med 29: 357–364.

Tan CB, Gao M, Xu WR, Yang XY, Zhu XM, Du GH (2009). Protective effects of salidroside on endothelial cell apoptosis induced by cobalt chloride. Biol Pharm Bull 32: 1359–1363.

Tang Y, Huang B, Sun L, Peng X, Chen X, Zou X (2011). Ginkgolide B promotes proliferation and functional activities of

bone marrow-derived endothelial progenitor cells: involvement of Akt/eNOS and MAPK/p38 signaling pathways. Eur Cell Mater 21: 459–469.

Tepper OM, Capla JM, Galiano RD, Ceradini DJ, Callaghan MJ, Kleinman ME *et al*. (2005). Adult vasculogenesis occurs through in situ recruitment, proliferation, and tubulization of circulating bone marrow-derived cells. Blood 105: 1068–1077.

Vasa M, Fichtlscherer S, Aicher A, Adler K, Urbich C, Martin H *et al*. (2001). Number and migratory activity of circulating endothelial progenitor cells inversely correlate with risk factors for coronary artery disease. Circ Res 89: E1–E7.

Verseijden F, Posthumus-van Sluijs SJ, Farrell E, van Neck JW, Hovius SE, Hofer SO *et al*. (2010). Prevascular structures promote vascularization in engineered human adipose tissue constructs upon implantation. Cell Transplant 19: 1007–1020.

Verseijden F, Posthumus-van Sluijs SJ, van Neck JW, Hofer SO, Hovius SE, van Osch GJ (2012). Vascularization of prevascularized and non-prevascularized fibrin-based human adipose tissue constructs after implantation in nude mice. J Tissue Eng Regen Med 6: 169–178.

Williams MR, Arthur JS, Balendran A, van der Kaay J, Poli V, Cohen P *et al*. (2000). The role of 3-phosphoinositide-dependent protein kinase 1 in activating AGC kinases defined in embryonic stem cells. Curr Biol 10: 439–448.

Wong BW, Rahmani M, Luo Z, Yanagawa B, Wong D, Luo H *et al*. (2009). Vascular endothelial growth factor increases human cardiac microvascular endothelial cell permeability to low-density lipoproteins. J Heart Lung Transplant 28: 950–957.

Xu MC, Shi HM, Wang H, Gao XF (2013). Salidroside protects against hydrogen peroxide-induced injury in HUVECs via the regulation of REDD1 and mTOR activation. Mol Med Rep 8: 147–153.

Zhai Z, Li H, Liu G, Qu X, Tian B, Yan W *et al*. (2013). Andrographolide suppresses RANKL-induced osteoclastogenesis *in vitro* and prevents inflammatory bone loss *in vivo*. Br J Pharmacol 171: 663–675.

Zhong H, Xin H, Wu LX, Zhu YZ (2010). Salidroside attenuates apoptosis in ischemic cardiomyocytes: a mechanism through a mitochondria-dependent pathway. J Pharmacol Sci 114: 399–408.